# FontHalu: Font-based Hallucinations in Multimodal Large Language Models

Anonymous ACL submission

## Abstract

Multimodal large language models (MLLMs) have achieved remarkable performance in processing and reasoning over text and images. However, they remain susceptible to hallucinations—instances where generated content deviates from input data or contradicts established knowledge. While extensive research has explored general hallucinations in MLLMs, font-induced hallucinations remain an overlooked yet critical challenge, particularly in OCR-based applications and high-stakes domains such as medical and legal text analysis. In this work, we formally define the phenomenon of font hallucinations and systematically categorize them into three types: font style, font semantics, and font sentiment. We further conduct comprehensive experimental analyses to quantify their impact on model reliability. Building on this analysis, we propose the FontHalu benchmark, the first dedicated benchmark for evaluating MLLMs' robustness against font-based hallucinations. To mitigate these hallucinations, we implement LoRA-based parameter-efficient fine-tuning, demonstrating improved generalization to unseen fonts while highlighting the limitations of current adaptation techniques. We will publicly release the benchmark and datasets, advancing the development of more reliable multimodal AI systems.

## 1 Introduction

Multimodal large language models (MLLMs) have significantly advanced text and image processing, yet they remain vulnerable to hallucinations (Bai et al., 2024a), where generated content deviates from input data or contradicts established knowledge, undermining their reliability. Existing studies have identified various forms of hallucinations in multimodal systems. For instance, Liu et al. (2024d) demonstrate that MLLMs can generate incorrect answers despite correctly interpreting visual content, using paired positive and negative visual question-answer samples. Similarly, PhD (Liu et al., 2024c) highlights significant variability in MLLM performance across different tasks, exposing inconsistencies in how these models reason over multimodal inputs.

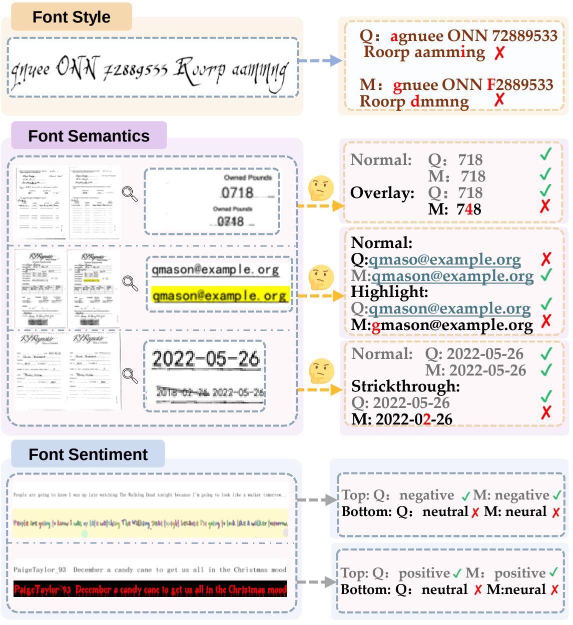
Font Style
gnuee ONN 72889533 Roorp aamming
Q: agnuee ONN 72889533 Roorp aamming ✗
M: gnuee ONN F2889533 Roorp dmmng ✗
Font Semantics
Owned Pounds
0718
Owned Pounds
0748
Normal: Q: 718 ✓
M: 718 ✓
Overlay: Q: 718 ✓
M: 748 ✗
qmason@example.org
qmason@example.org
Normal:
Q:qmaso@example.org ✗
M:qmason@example.org ✓
Highlight:
Q:qmason@example.org ✓
M:gmason@example.org ✗
2022-05-26
2018-02-24 2022-05-26
Normal: Q: 2022-05-26 ✓
M: 2022-05-26 ✓
Strickthrough:
Q: 2022-05-26 ✓
M: 2022-02-26 ✗
Font Sentiment
People are going to know I was up late watching The Walking Dead tonight because I'm going to look like a walker tomorrow...
Top: Q: negative ✓ M: negative ✓
Bottom: Q: neutral ✗ M: neural ✗
PaigeTaylor_93 December a candy cane to get us all in the Christmas mood
Top: Q: positive ✓ M: positive ✓
Bottom: Q: neutral ✗ M:neural ✗

Figure 1: Examples of font-related hallucinations in MLLMs: a case study of Qwen2-VL-7B (Q) and MiniCPM-V-2.6 (M). The letters marked in red indicate those that are inconsistent with the ground truth.

While extensive research has explored general hallucinations in MLLMs, the interaction between textual and visual features introduces additional challenges. In particular, font styles and sizes can significantly affect MLLMs' perception of textual information. As shown in Figure 1, changes in font style may cause MLLMs to confuse visually similar letters during text recognition. Furthermore, stylistic variations can alter the perceived sentiment of a text, resulting in misclassification in sentiment analysis. We define this phenomenon as

FontHalu—errors or unreasonable outputs generated by MLLMs due to the visual characteristics of fonts within input images, rather than the textual semantics alone.

FontHalu is not merely an academic concern but pose tangible risks in real-world applications. For example, in *medical diagnostics*, font misinterpretations in patient records may result in incorrect treatments, while in *legal document processing*, hallucinations could lead to misread contract clauses with significant consequences. Although the increasing reliance on MLLMs for automated document understanding, the effects of font variations remain largely unexplored, leaving a critical gap in model robustness evaluation.

Despite the significance of this issue, existing benchmarks fail to systematically assess the impact of font hallucinations on model reliability. CHAIR (Rohrbach et al., 2018) and POPE (Li et al., 2023c) evaluates object hallucination. OCRbench (Liu et al., 2024e), SROIE (Huang et al., 2021), DOCVQA (Mathew et al., 2021), TextVQA (Singh et al., 2019) primarily evaluate OCR performance. While some benchmarks include recognition of handwritten or artistic fonts (Cui et al., 2024), they cover only a limited range of font variations and do not systematically investigate font-based hallucinations, leaving an important gap in MLLMs evaluation.

To address this gap, we adopt a controlled variable methodology to systematically analyze MLLM performance across multiple dimensions of font variation. Specifically, we investigate how models respond to changes in font attributes, font types, and more complex typographic transformations. These carefully designed experiments provide valuable insights into the challenges posed by font-based hallucinations. Based on these findings, we introduce the FontHalu benchmark—the first dedicated benchmark for evaluating MLLMs' robustness against font-based hallucinations. Our contributions are as follows:

1. We introduce the FontHalu phenomenon, categorize its types, and conduct a detailed empirical analysis to characterize its impact on MLLMs.

2. We develop FontHalu benchmark, the first benchmark specifically designed to systematically evaluate font-induced hallucinations in MLLMs, enabling standardized assessment and comparison.

3. We construct a specialized training dataset for fine-tuning MLLMs, incorporating font-specialized modifications to mitigate font-based hallucinations and enhance model reliability in font-related tasks.

## 2 Related Work

**Hallucinations in MLLMs** The remarkable success of LLMs has paved the way for the development of multimodal large language model (Li et al., 2023a; Liu et al., 2024b; Wang et al., 2024; Zhu et al., 2024), which combine pretrained visual models with LLMs to enable their visual capabilities. But at the same time, it also introduced many vision specific hallucination phenomena (Gunjal et al., 2024; Jiang et al., 2024; Zhou et al., 2024). These hallucinations can be roughly classified into category, attribute, and relationship (Bai et al., 2024b). In the research on category types (Liu et al., 2024a; Yu et al., 2024) mainly focuses on object existence and descriptive issues, while research on fonts is relatively scarce. However, fonts play a crucial role in tasks such as KIE (Knowledge-Intensive Extraction) recognition, text-guided VQA (Visual Question Answering) tasks, and sentiment analysis tasks (Liu et al., 2023; Huang et al., 2021; Mathew et al., 2021; Singh et al., 2019). Therefore, studying the hallucinations problem caused by fonts is of great significance and can promote further development in the field of MLLM hallucinations.

**Benchmarks for MLLMs** There are many hallucination benchmarks for MLLMs, such as POPE (Li et al., 2023b), Nope (Lovenia et al., 2023), and CIEM (Hu et al., 2023). While effective for basic hallucination assessment, these benchmarks notably exclude OCR recognition capabilities from their evaluation scope (Liu et al., 2024a; Chen et al., 2023). Recently, more and more hallucination benchmarks have mentioned OCR recognition as an important part of multimodal hallucination assessment, such as HallusionBench (Guan et al., 2024) and MME (Cui et al., 2024). However, their treatment of OCR-related hallucinations is limited, particularly in addressing the impact of font variations on hallucinations in MLLMs, a factor that can significantly affect recognition accuracy.

## 3 Font-based Hallucinations

In this work, we identify three typical types of FontHalu: hallucinations of font style, hallucina-

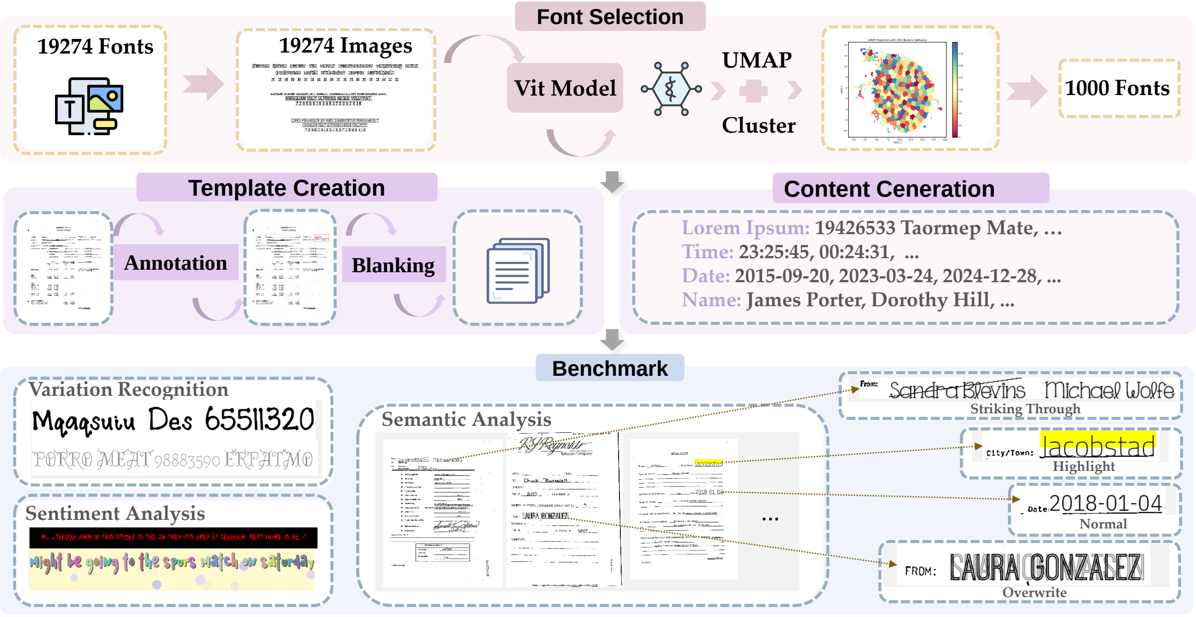

Figure 2: The constructions pipeline of benchmark.

tions of font semantics, and hallucinations of font sentiment.

**Hallucinations of Font Style** From the perspective of a single font, Shimoda et al. (2024) divide font attributes into various aspects, such as color, alignment, capitalization, font size, angle, letter spacing, and line height. Additionally, Brown (2024) categorizes font variation axes into six dimensions: weight, width, slant, italic, optical size, and X-height. In this work, we focus on six key dimensions of font attributes: size, spacing, slant, alignment, weight, and X-height.

- **Size**: Adjusts the font size, ranging from small to large.
- **Spacing**: Varies the space between letters, from tight to loose.
- **Slant**: Changes the font's angle, tilting letters to the right without altering their forms.
- **Alignment**: Determines text alignment, from left to right or center.
- **Weight**: Adjusts stroke thickness, ranging from light to bold.
- **Line-height**: Controls the vertical space between text lines.

The combination of dimensional variations results in style changes within the same font. From the perspective of different font families, font styles can vary widely, including categories such as Serif (Arditi and Cho, 2005), Sans-Serif, Script, Monospaced, and others characterized by unique features like strokes. These varying font styles affect MLLMs' ability to accurately recognize text, leading to differences in performance across font types. We refer to this phenomenon as Font Style Hallucinations. For instance, transitioning from a standard typeface to a more decorative or handwritten style can cause the model to misinterpret the text, potentially leading to hallucinations and incorrect inferences. In Figure 1, for example, the model confuses '7' with 'F' and 'g' with 'q' due to the specific font. This misinterpretation often manifests in the confusion of visually similar characters, which is exacerbated by stylistic elements.

**Hallucinations of Font Semantics** In practical applications, adjustments to font style can introduce additional semantic cues or nuances to the text. For example, highlighting a word serves to emphasize its importance. Wu and Yuan (2003) find that highlighting can significantly improve table search efficiency. In handwritten documents, strike-through text may appear, potentially complicating OCR system recognition (Adak and Chaudhuri, 2014). This is particularly relevant since striking through a word and replacing it with a new one signifies that the original term is invalid and has been superseded. Additionally, overlay text plays a vital role in video content analysis, providing key semantic cues for tasks such as video information retrieval and summarization (Adak and Chaudhuri, 2014). Similarly, when a word is written in a light color and overlaid with a darker one, the darker color often conveys the final or correct answer. However, MLLMs may not always be capable of recognizing these semantic cues, leading to hallucinations, which we refer to as Font Semantics Hallucinations. As shown in Figure 1, MiniCPM treats the strikethrough text as the final answer, resulting in a semantic hallucination.

**Hallucinations of Font Sentiment** Emotion-driven attention facilitation is influenced not only by biological relevance but also by perceptual features, such as font size (Bayer et al., 2012). In this context, Zhang et al. (2018) used semantic differential and statistical analysis methods to identify factors like exquisiteness, constriction, and a sense of order, which shape the emotional perception of fonts. For example, fonts themselves can evoke emotional tones, such as the horror effect conveyed by the *Silent Hill* font. This raises the question: **do MLLMs recognize these emotional cues in fonts?** If so, they may misinterpret or exaggerate the emotional tone, resulting in what we term Font Sentiment Hallucinations. As shown in Figure 1, the models can correctly assess sentiment with a neutral (or standard) font. However, when we switch to a more cheerful-looking font, the models' response changes from negative to neutral. Similarly, when the models assess sentiment as positive in a neutral font, switching to a horror-themed font causes the sentiment evaluation to shift to neutral, resulting in a font sentiment hallucination.

We will experimentally validate and analyze the aforementioned hallucinations in Section 5.1.

# 4 FontHalu Benchmark

## 4.1 Overview

The FontHalu benchmark is a comprehensive evaluation framework designed to assess the impact of font-induced hallucinations on MLLM. This benchmark specifically targets the three types of font hallucinations introduced earlier: Font Style, Font Semantics, and Font Sentiment. To systematically evaluate these phenomena, we introduce three dedicated sub-tasks:

- **Font Variation Recognition (VarRec)**: This task involves extracting text rendered in different fonts from images with a blank background. It aims to measure the model's robustness to font variations in isolated text recognition scenarios.

- **Font Semantic Analysis (SemAna)**: This task evaluates the model's ability to extract text from real-world contexts, such as shipping labels or documents, where additional semantic cues—such as strikethroughs, highlights, or overlays—may alter the intended meaning.

- **Font Sentiment Analysis (SentAna)**: This task assesses the extent to which a model can correctly interpret the sentiment of a sentence when presented in a specific font, reflecting the potential influence of typography on sentiment perception.

## 4.2 Construction

The benchmark construction process, illustrated in Figure 2, consists of four key stages: font selection, image template creation, content generation, and benchmark assembly.

**Font Selection** In this stage, we collect a diverse set of fonts, including both commonly used and rare artistic or commercial fonts, to ensure comprehensive coverage of font variations. Ultimately, we gather 19,274 distinct fonts, each applied to render identical content on $250 \times 1500$ pixel blank images. The content consists of two lines of Lorem Ipsum text and one line of numerical data, generating a total of 19,274 images. These images are then processed using a pre-trained ViT model (ViT-Base-Patch16-224) (Dosovitskiy et al., 2021) to extract feature vectors from the final hidden layer. To reduce dimensionality, we apply UMAP (McInnes and Healy, 2018), followed by K-means clustering (Lloyd, 1982) to group the feature vectors into 200 clusters. From each cluster, five representative fonts are selected, yielding a total of 1,000 candidate fonts for the benchmark[1].

**Template Creation** In this phase, 200 images are selected from publicly available datasets, including DocVQA (Mathew et al., 2021), FUNSD (Jaume et al., 2019) and SROIE (Huang et al., 2021)[2].

[1] For a detailed explanation of the font selections algorithm,see appendix A.

[2] In this paper, all publicly available datasets used have been authorized and strictly adhere to the relevant usage agreements.

We then annotate each image with 2–3 bounding boxes (annotation criteria are shown in Appendix B). To facilitate controlled content placement, we binarize these images by removing the content within the annotated regions while preserving the location information. This process results in 200 annotated template images.

**Content Generation** In this phase, we design various data types based on the annotated bounding boxes, including Lorem Ipsum text, numbers, dates, times, names, addresses, email addresses, etc. These content types are selected to reflect diverse real-world text data, ensuring broad scenario coverage.

For each task, we follow specific content generation strategies: **VarRec Task:** The selected fonts are used to write Lorem Ipsum content on blank images. **SemAna Task:** Questions are first generated based on the key information associated with the annotated bounding boxes in the image templates. Then, specific content is written in these bounding boxes using various fonts while applying one of four randomly selected formatting modes: strikethrough, highlighting, overlay, or normal. These modified texts serve as our ground-truth answers. **SentAna Task:** The test set of the `Sentiment140` dataset is rendered in different fonts.

Finally, we manually verify the dataset, removing low-quality samples to ensure data integrity (the specific criteria are shown in Appendix B). This results in the final version of the FontHalu benchmark. Statistics of the FontHalu benchmark are presented in Table 1.

| Task | Images | Questions |
|---|---|---|
| **VarRec** | 250 | 250 |
| **SemAna** | 780 | 1877 |
| Normal | 589 | 928 |
| Strikethrough | 124 | 132 |
| Overlay | 317 | 393 |
| Highlight | 343 | 424 |
| **SentAna** | 200 | 200 |

Table 1: Task overview: number of images and questions. Normal, Strikethrough, Overlay, and Highlight refer to the four types of text formatting in the SemAna task.

### 4.3 Evaluation Metrics

We evaluate MLLMs' performance using the following metrics: **ACC:** Measures the presence of the expected answer in the generated response, with higher values indicating better performance. **NED:** Measures the normalized edit distance between the expected and generated answers, with lower values indicating better performance[3].

## 5 Experiments

### 5.1 Font-based Hallucinations

To validate the three types of hallucinations introduced in Section 3, we design targeted experiments to analyze the characteristics and manifestations of FontHalu. For detailed experimental settings, refer to Appendix D.

**Settings** When investigating **hallucinations of font style**, we first explore the variations in font attributes using a single, commonly used font. These attributes include size (ranging from 15 to 50 pt), spacing (from -0.1 to 0.4 em), slant (from 15 to 50 degrees), alignment (left, center, right), weight (from 100 to 900 on the font weight scale), and line height (from 0.4 to 2.0 em). To minimize potential confounding factors, we present the font against a plain background, avoiding any layout or contextual influences. This experiment is referred to as **Font Style (Plain)**. Next, we examine the impact of different font types, using five distinct fonts. To simulate real-world scenarios more effectively, we incorporate these fonts into contextual settings (such as tracking numbers and receipts). This experiment, conducted on both Chinese and English datasets, is called **Font Style (Scene)**.

For **hallucinations of font semantics**, We examine how MLLMs interpret content when text is presented in four different formatting styles: normal, overlay, highlight, and strikethrough. We refer to this experiment as **Font Semantics**.

We further examine how MLLMs exhibit **hallucinations of font sentiment** when presented with identical content rendered in five different fonts: a visually neutral font (NF), two horror-themed fonts (HF-A, HF-B), and two visually cheerful fonts (CF-A, CF-B)[4]. We refer to this experiment as **Font Sentiment**.

The hyperparameters for the models used in these experiments remain at their default settings.[5]

[3] Specific calculation formulas are in the appendix C.

[4] Figure 8 illustrates the five fonts separately.

[5] For detailed configuration parameters, please refer to the website `https://huggingface.co`.

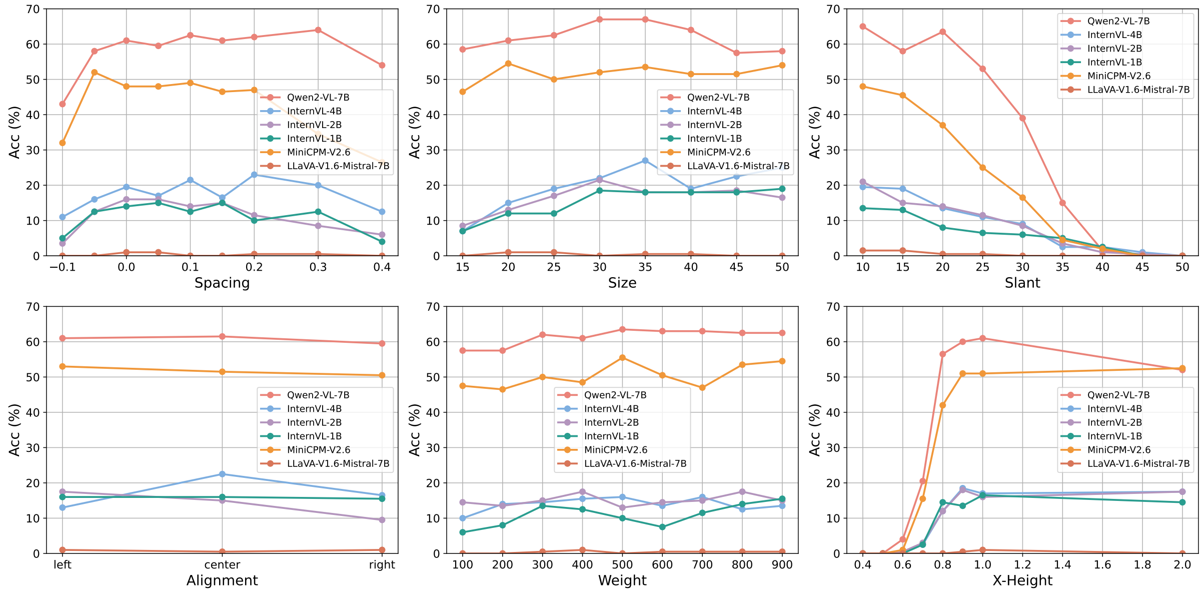

Figure 3: Results on font variations for text recognition using MLLMs with plain backgrounds.

| **Model** | 0–9 | | 0–9 | | 0–9 | | 0–9 | | 0-9 | |
|---|---|---|---|---|---|---|---|---|---|---|
| | **ACC** | **NED** | **ACC** | **NED** | **ACC** | **NED** | **ACC** | **NED** | **ACC** | **NED** |
| | | | | | English Dataset | | | | | |
| Qwen2-VL-7B | 25.90% | 0.48 | **62.10%** | 0.56 | 45.10% | 0.45 | 59.00% | 0.31 | 57.90% | 0.33 |
| InternVL-1B | 32.00% | 0.34 | 28.70% | 0.42 | 49.80% | 0.28 | 48.50% | 0.31 | **50.10%** | 0.28 |
| InternVL-2B | 23.70% | 0.22 | 25.20% | 0.28 | **45.10%** | 0.12 | 41.10% | 0.13 | 42.10% | 0.13 |
| InternVL-4B | 25.00% | 0.31 | 13.20% | 0.41 | 36.50% | 0.28 | 32.10% | 0.31 | **38.20%** | 0.27 |
| MiniCPM-V2.6 | 43.20% | 0.10 | 30.90% | 0.23 | **73.60%** | 0.05 | 68.20% | 0.05 | 73.20% | 0.05 |
| LLaVA-V1.6-Mistral-7B | 0.00% | 0.79 | 0.00% | 0.83 | 0.00% | 0.72 | 0.00% | 0.77 | 0.00% | 0.78 |
| | | | | | Chinese Dataset | | | | | |
| Qwen2-VL-7B | 75.30% | 0.12 | 62.10% | 0.13 | 80.00% | 0.10 | 83.80% | 0.08 | **84.80%** | 0.06 |
| InternVL-1B | 17.80% | 0.42 | 18.00% | 0.52 | **37.10%** | 0.36 | 34.20% | 0.38 | 34.50% | 0.38 |
| InternVL-2B | 21.70% | 0.23 | 17.60% | 0.29 | 32.10% | 0.17 | 31.70% | 0.19 | **42.10%** | 0.18 |
| InternVL-4B | 42.50% | 0.11 | 44.60% | 0.16 | **69.10%** | 0.07 | 63.00% | 0.09 | 62.50% | 0.08 |
| MiniCPM-V2.6 | 41.00% | 0.16 | 25.30% | 0.21 | 65.40% | 0.08 | **66.40%** | 0.08 | 64.40% | 0.09 |

Table 2: The effect of font variations on scene text recognition using MLLMs for both English and Chinese datasets. Bold purple indicates the highest score across five fonts. The fonts from left to right are: *Debiao Pen Calligraphy*, *FZCYFW*, *Luxi Mono*, *Bold Oblique*, *Liugongquan Calligraphy*, and *IBMPlexSerif-LightItalic*.

| **Model** | **Normal** | | **Overlay** | | **Highlight** | | **Strikethrough** | |
|---|---|---|---|---|---|---|---|---|
| | **ACC** | **NED** | **ACC** | **NED** | **ACC** | **NED** | **ACC** | **NED** |
| Qwen2-VL-7B | 85.89% | 0.12 | 50.62%$^-$ | 0.23 | 86.38%$^+$ | 0.11 | 60.18%$^-$ | 0.61 |
| MiniCPM-V2.6 | 90.09% | 0.07 | 50.62%$^-$ | 0.18 | 92.68%$^+$ | 0.06 | 75.00%$^-$ | 0.55 |
| InternVL-1B | 76.70% | 0.18 | 39.55%$^-$ | 0.32 | 79.11%$^+$ | 0.16 | 52.90%$^-$ | 0.62 |
| InternVL-2B | 77.86% | 0.15 | 39.11%$^-$ | 0.29 | 77.23%$^-$ | 0.13 | 51.70%$^-$ | 0.62 |
| InternVL-4B | 81.56% | 0.12 | 43.97%$^-$ | 0.25 | 82.68%$^+$ | 0.10 | 64.38%$^-$ | 0.57 |
| LLaVA-V1.6-Mistral-7B | 66.25% | 0.65 | 33.26%$^-$ | 0.73 | 66.52%$^+$ | 0.63 | 35.89%$^-$ | 0.84 |

Table 3: Evaluation of MLLMs for font semantics understanding. $^-$ indicates a score decrease relative to Normal, while $^+$ indicates an increase.

**Results** The experimental results for **Font Style (Plain)** are shown in Figure 3. These findings suggest that even minor adjustments to a specific font dimension, while keeping the textual content unchanged, can significantly impact the recognition performance of MLLMs. The results of the **Font**

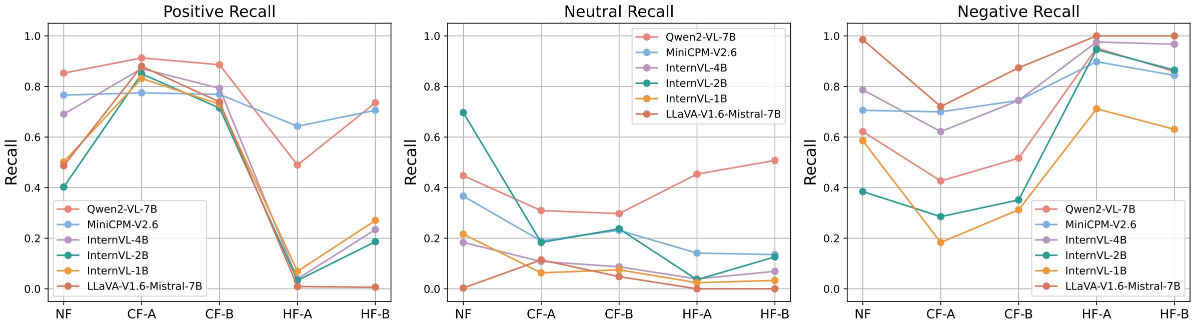

Figure 4: Impact of font variations on sentiment analysis with MLLMs: Example Images in Appendix D.

**Style (Scene)** experiment, shown in Table 2, indicate that font style variations can lead to inconsistent recognition outcomes in MLLMs, even with constant textual content. Different MLLMs also have varying preferences for specific font styles.

The results for **Font Semantics** in Table 3 show that highlighting improves MLLMs' performance, while Overlay and Strikethrough reduce recognition scores compared to the Normal condition. This indicates that certain font-based modifications can obscure textual cues, leading to increased hallucination rates. The **Font Sentiment** results in Figure 4 show that cheerful fonts (CF-A/B) boost positive recall, while horror fonts (HF-A/B) increase negative recall. The Neutral font (NF) yields the highest neutral recall for most models, except Qwen2-VL-7B and LLaVA-V1.6-Mistral-7B. These findings highlight that font variations influence sentiment classification in MLLMs, reinforcing the need for robustness against font-induced sentiment shifts.

### 5.2 Benchmarking of MLLMs using FontHalu

We evaluated 30 models, including both open-source and proprietary advanced MLLMs, on the FontHalu benchmark. A detailed list of model names and sources can be found in Appendix F.

**Settings** Following OCRbench (Liu et al., 2024e), the FontHalu benchmark adopts a question-answering (QA) format, enabling efficient evaluation of models' capabilities. The querying prompts for each subtask are as follows: **VarRec**: "What's the content in the image? Only return the content." **SemAna**: "What's the {key} in the image? Only return the {key}." **SentAna**: "What emotions do the text in the picture express? Choose one from ['positive', 'negative', 'neutral']." All model parameters remain consistent with their official configurations, and API calls follow the same settings as the online versions to ensure reproducibility.

**Results** The evaluation results on the FontHalu benchmark are summarized in Table 4, where Qwen2-VL-7B achieves the highest score, followed by Qwen2-VL-2B in second place. Figure 5 visualizes the performance differences among the top six models across the three sub-tasks. Notably, substantial variations are observed in the VarRec and SemAna sub-tasks. The Qwen series models demonstrate the best performance in VarRec, while GPT-4o achieves the highest accuracy in SemAna.

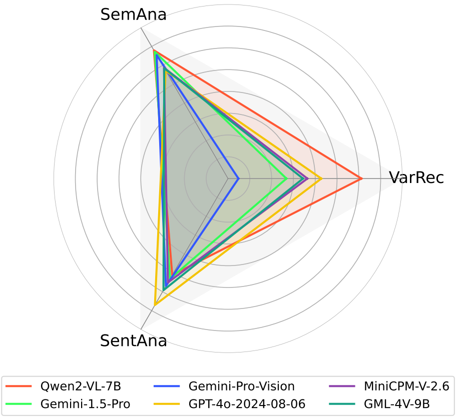

Figure 5: Comparison of the ACC scores of the top 6 MLLMs across 3 subtasks. Detailed ACC scores of all models on three subtasks can be found in Appendix E.

### 5.3 Mitigation Strategies

We hypothesize that FontHalu in MLLMs arises due to insufficient exposure to diverse fonts during training, leading to poor generalization to unseen fonts. To test this, we use fine-tuning to mitigate FontHalu in this experiment.

**Settings** We first create a training dataset (*Same*) using 687 fonts that are included in the benchmark, ensuring the model encounters the same fonts during training and testing. Then we investigate the model's ability to generalize to unseen fonts. We

| Name | ACC | Name | ACC |
|---|---|---|---|
| Qwen2-VL-7B | 0.6649 | Pixtral-12B | 0.4872 |
| Qwen2-VL-2B | 0.6558 | InternVL2-8B | 0.4857 |
| Gemini-1.5-Pro | 0.6148 | InternVL2-1B | 0.4849 |
| Gemini-Pro-Vision | 0.5816 | InternVL2-2B | 0.4798 |
| GPT-4o-2024-08-06 | 0.5661 | CogVLM2-LLaMA3-19B-Chat | 0.4616 |
| MiniCPM-V-2.6 | 0.5601 | LLaMA3.2-90B-Vision-Instruct | 0.4359 |
| GML-4V-9B | 0.5599 | Phi3.5-Vision-Instruct | 0.4218 |
| Phi-3-Vision-128k-Instruct | 0.5527 | Ovis1.5-LLaMA3-8B | 0.3879 |
| InternVL2.5-1B | 0.5517 | LLaVA-V1.6-Vicuna-7B-hf | 0.3805 |
| InternVL2.5-2B | 0.5509 | LLaMA3-LLaVA-Next-8B-hf | 0.3647 |
| Qwen2-VL-72B-Instruct | 0.5499 | LLaVA-V1.6-Mistral-7B | 0.3597 |
| InternVL2-4B | 0.5306 | LLaMA3.2-11B-Vision-Instruct | 0.2866 |
| InternVL2.5-8B | 0.5259 | DeepSeek-VL-7B-Chat | 0.2339 |
| InternVL2.5-4B | 0.5251 | InstructBLIP-Vicuna-7B | 0.0349 |
| MiniMax-01 | 0.4910 | BLIP-VQA-Base | 0.0284 |

Table 4: Overall performance of MLLMs on benchmark. The scores are arranged in descending order, from top to bottom, and from left to right.

create two additional datasets: *Cluster-200* with 687 fonts from 200 clusters (excluding benchmark fonts) and *Cluster-10* (excluding benchmark fonts) with 687 fonts from the top 10 clusters. Each font in the training sets is used to generate 10 images, resulting in 6,870 samples per set. During evaluation, we first test the models on the benchmark dataset. Then, we assess performance on a more diverse test set of 10,000 distinct fonts, excluding those used in training. All test images are generated with Lorem Ipsum text on a blank background[6].

**Results** The results in Table 5 show that training MLLMs with benchmark fonts improves performance, reducing hallucinations. Training with clustered fonts also helps, indicating the model's ability to generalize across different fonts. However, the Qwen2-VL-7B model's performance drops with the *Same* or *Cluster-200* datasets, which may be attributed to the model's parameterization being unsuitable for uniform training samples, resulting in overfitting to specific font styles. Although font category coverage during training has minimal impact on benchmark performance, the table also shows that training with 200 font clusters generally results in better performance on the test set compared to training with only 10 clusters.

| Model | B-ACC | T-ACC |
|---|---|---|
| LLaVA-V1.6-Mistral-7B | 0.3588 | 0.0166 |
| *Same* | 0.3866↑ | 0.2344 |
| *Cluster-10* | 0.3876↑ | 0.2357 |
| *Cluster-200* | 0.3821↑ | **0.2466** |
| MiniCPM-V-2.6 | 0.5576 | 0.2690 |
| *Same* | 0.5932↑ | 0.3995 |
| *Cluster-10* | 0.5923↑ | 0.3851 |
| *Cluster-200* | 0.6066↑ | **0.4020** |
| Qwen2-VL-7B | 0.6649 | 0.5905 |
| *Same* | 0.6595↓ | 0.7244 |
| *Cluster-10* | 0.6671↑ | 0.7097 |
| *Cluster-200* | 0.6561↓ | **0.7245** |

Table 5: Performance comparison of MLLMs on benchmark(B-ACC) and test datasets(T-ACC). Bold denotes the highest-performing method under a specific model, while underlined denotes the second-highest performing method.

## 6 Conclusion

This paper explores font hallucinations in MLLMs, investigating their impact across style, semantics, and sentiment. To address the lack of dedicated evaluation frameworks, we develop the FontHalu benchmark, a comprehensive dataset designed to assess MLLMs' robustness to font-induced hallucinations. Our extensive experiments reveal that even minor typographic variations can significantly alter model predictions, underscoring the need for greater font awareness in multimodal AI systems. Beyond benchmarking, we explore mitigation strategies by constructing specialized training datasets and applying parameter-efficient finetuning techniques. Our results demonstrate that exposure to a diverse set of fonts during training improves generalization, reducing hallucination rates. By systematically investigating FontHalu, we provide a foundation for developing more reliable, interpretable, and font-aware multimodal large language models, paving the way for AI systems that perform robustly across diverse typographic contexts.

[6] Training parameters are detailed in Appendix G.

## Limitations

This study categorizes FontHalu into three distinct types, providing a useful framework for understanding font-related hallucinations. However, we acknowledge that this classification may not be exhaustive and could benefit from further exploration of additional categories. As font-induced hallucinations are an emerging research area, further studies are needed to refine and expand upon this taxonomy.

Furthermore, although we cluster over 19,000 fonts and thoughtfully select 1,000 fonts for our benchmark, aiming to cover a wide range of typographic styles. However, we recognize that even with this selection, the full diversity of font styles may not be fully captured, and there is potential for expanding its scope. Font variations are virtually limitless, spanning different scripts, handwritten styles, and dynamically generated typefaces, which pose additional challenges not addressed in this study.

Additionally, while we explore mitigation strategies through fine-tuning, our approach does not investigate alternative methods such as in-context learning, prompt engineering, or reinforcement learning, which may offer more effective or generalizable solutions. Future research could explore these techniques to further enhance MLLMs' robustness against font-induced hallucinations.

## References

Chandranath Adak and Bidyut B. Chaudhuri. 2014. An approach of strike-through text identification from handwritten documents. In *2014 14th International Conference on Frontiers in Handwriting Recognition*, pages 643–648.

Aries Arditi and Jianna Cho. 2005. Serifs and font legibility. *Vision research*, 45(23):2926–2933.

Zechen Bai, Pichao Wang, Tianjun Xiao, Tong He, Zongbo Han, Zheng Zhang, and Mike Zheng Shou. 2024a. Hallucination of multimodal large language models: A survey. *ArXiv*, abs/2404.18930.

Zechen Bai, Pichao Wang, Tianjun Xiao, Tong He, Zongbo Han, Zheng Zhang, and Mike Zheng Shou. 2024b. Hallucination of multimodal large language models: A survey. *CoRR*, abs/2404.18930.

Mareike Bayer, Werner Sommer, and Annekathrin Schacht. 2012. Font size matters—emotion and attention in cortical responses to written words. *PloS one*, 7(5):e36042.

Nik Bear Brown. 2024. The cognitive type project - mapping typography to cognition. *ArXiv*, abs/2403.04087.

Zhiyang Chen, Yousong Zhu, Yufei Zhan, Zhaowen Li, Chaoyang Zhao, Jinqiao Wang, and Ming Tang. 2023. Mitigating hallucination in visual language models with visual supervision. *CoRR*, abs/2311.16479.

Can Cui, Yunsheng Ma, Xu Cao, Wenqian Ye, Yang Zhou, Kaizhao Liang, Jintai Chen, Juanwu Lu, Zichong Yang, Kuei-Da Liao, Tianren Gao, Erlong Li, Kun Tang, Zhipeng Cao, Tong Zhou, Ao Liu, Xinrui Yan, Shuqi Mei, Jianguo Cao, Ziran Wang, and Chao Zheng. 2024. A survey on multimodal large language models for autonomous driving. In *IEEE/CVF Winter Conference on Applications of Computer Vision Workshops, WACVW 2024 - Workshops, Waikoloa, HI, USA, January 1-6, 2024*, pages 958–979. IEEE.

Alexey Dosovitskiy, Lucas Beyer, Alexander Kolesnikov, Dirk Weissenborn, Xiaohua Zhai, Thomas Unterthiner, Mostafa Dehghani, Matthias Minderer, Georg Heigold, Sylvain Gelly, Jakob Uszkoreit, and Neil Houlsby. 2021. An image is worth 16x16 words: Transformers for image recognition at scale. In *9th International Conference on Learning Representations, ICLR 2021, Virtual Event, Austria, May 3-7, 2021*. OpenReview.net.

Tianrui Guan, Fuxiao Liu, Xiyang Wu, Ruiqi Xian, Zongxia Li, Xiaoyu Liu, Xijun Wang, Lichang Chen, Furong Huang, Yaser Yacoob, Dinesh Manocha, and Tianyi Zhou. 2024. Hallusionbench: An advanced diagnostic suite for entangled language hallucination and visual illusion in large vision-language models. In *Proceedings of the IEEE/CVF Conference on Computer Vision and Pattern Recognition (CVPR)*, pages 14375–14385.

Anisha Gunjal, Jihan Yin, and Erhan Bas. 2024. Detecting and preventing hallucinations in large vision language models. In *Thirty-Eighth AAAI Conference on Artificial Intelligence, AAAI 2024, Thirty-Sixth Conference on Innovative Applications of Artificial Intelligence, IAAI 2024, Fourteenth Symposium on Educational Advances in Artificial Intelligence, EAAI 2014, February 20-27, 2024, Vancouver, Canada*, pages 18135–18143. AAAI Press.

Hongyu Hu, Jiyuan Zhang, Minyi Zhao, and Zhenbang Sun. 2023. CIEM: contrastive instruction evaluation method for better instruction tuning. *CoRR*, abs/2309.02301.

Zheng Huang, Kai Chen, Jianhua He, Xiang Bai, Dimosthenis Karatzas, Shijian Lu, and C. V. Jawahar. 2021. ICDAR2019 competition on scanned receipt OCR and information extraction. *CoRR*, abs/2103.10213.

Guillaume Jaume, Hazim Kemal Ekenel, and Jean-Philippe Thiran. 2019. FUNSD: A dataset for form understanding in noisy scanned documents. *CoRR*, abs/1905.13538.

Chaoya Jiang, Hongrui Jia, Mengfan Dong, Wei Ye, Haiyang Xu, Ming Yan, Ji Zhang, and Shikun Zhang. 2024. Hal-eval: A universal and fine-grained hallucination evaluation framework for large vision language models. In *Proceedings of the 32nd ACM International Conference on Multimedia*, pages 525–534.

Junnan Li, Dongxu Li, Silvio Savarese, and Steven C. H. Hoi. 2023a. BLIP-2: bootstrapping language-image pre-training with frozen image encoders and large language models. In *International Conference on Machine Learning, ICML 2023, 23-29 July 2023, Honolulu, Hawaii, USA*, volume 202 of *Proceedings of Machine Learning Research*, pages 19730–19742. PMLR.

Yifan Li, Yifan Du, Kun Zhou, Jinpeng Wang, Wayne Xin Zhao, and Ji-Rong Wen. 2023b. Evaluating object hallucination in large vision-language models. In *Proceedings of the 2023 Conference on Empirical Methods in Natural Language Processing, EMNLP 2023, Singapore, December 6-10, 2023*, pages 292–305. Association for Computational Linguistics.

Yifan Li, Yifan Du, Kun Zhou, Jinpeng Wang, Xin Zhao, and Ji-Rong Wen. 2023c. Evaluating object hallucination in large vision-language models. In *Proceedings of the 2023 Conference on Empirical Methods in Natural Language Processing*, pages 292–305, Singapore. Association for Computational Linguistics.

Fuxiao Liu, Kevin Lin, Linjie Li, Jianfeng Wang, Yaser Yacoob, and Lijuan Wang. 2024a. Mitigating hallucination in large multi-modal models via robust instruction tuning. In *The Twelfth International Conference on Learning Representations, ICLR 2024, Vienna, Austria, May 7-11, 2024*. OpenReview.net.

Haotian Liu, Chunyuan Li, Qingyang Wu, and Yong Jae Lee. 2024b. Visual instruction tuning. *Advances in neural information processing systems*, 36.

Jiazhen Liu, Yuhan Fu, Ruobing Xie, Runquan Xie, Xingwu Sun, Fengzong Lian, Zhanhui Kang, and Xirong Li. 2024c. Phd: A chatgpt-prompted visual hallucination evaluation dataset. *Preprint*, arXiv:2403.11116.

Yexin Liu, Zhengyang Liang, Yueze Wang, Muyang He, Jian Li, and Bo Zhao. 2024d. Seeing clearly, answering incorrectly: A multimodal robustness benchmark for evaluating mllms on leading questions. *Preprint*, arXiv:2406.10638.

Yuliang Liu, Zhang Li, Mingxin Huang, Biao Yang, Wenwen Yu, Chunyuan Li, Xu-Cheng Yin, Cheng-Lin Liu, Lianwen Jin, and Xiang Bai. 2024e. Ocrbench: on the hidden mystery of ocr in large multimodal models. *Science China Information Sciences*, 67(12).

Yuliang Liu, Zhang Li, Hongliang Li, Wenwen Yu, Mingxin Huang, Dezhi Peng, Mingyu Liu, Mingrui Chen, Chunyuan Li, Lianwen Jin, and Xiang Bai. 2023. On the hidden mystery of OCR in large multimodal models. *CoRR*, abs/2305.07895.

Stuart P. Lloyd. 1982. Least squares quantization in PCM. *IEEE Trans. Inf. Theory*, 28(2):129–136.

Holy Lovenia, Wenliang Dai, Samuel Cahyawijaya, Ziwei Ji, and Pascale Fung. 2023. Negative object presence evaluation (NOPE) to measure object hallucination in vision-language models. *CoRR*, abs/2310.05338.

Minesh Mathew, Dimosthenis Karatzas, and C. V. Jawahar. 2021. Docvqa: A dataset for VQA on document images. In *IEEE Winter Conference on Applications of Computer Vision, WACV 2021, Waikoloa, HI, USA, January 3-8, 2021*, pages 2199–2208. IEEE.

Leland McInnes and John Healy. 2018. UMAP: uniform manifold approximation and projection for dimension reduction. *CoRR*, abs/1802.03426.

Anna Rohrbach, Lisa Anne Hendricks, Kaylee Burns, Trevor Darrell, and Kate Saenko. 2018. Object hallucination in image captioning. In *Proceedings of the 2018 Conference on Empirical Methods in Natural Language Processing*, pages 4035–4045, Brussels, Belgium. Association for Computational Linguistics.

Wataru Shimoda, Daichi Haraguchi, Seiichi Uchida, and Kota Yamaguchi. 2024. Towards diverse and consistent typography generation. In *Proceedings of the IEEE/CVF Winter Conference on Applications of Computer Vision (WACV)*, pages 7296–7305.

Amanpreet Singh, Vivek Natarajan, Meet Shah, Yu Jiang, Xinlei Chen, Dhruv Batra, Devi Parikh, and Marcus Rohrbach. 2019. Towards VQA models that can read. In *IEEE Conference on Computer Vision and Pattern Recognition, CVPR 2019, Long Beach, CA, USA, June 16-20, 2019*, pages 8317–8326. Computer Vision Foundation / IEEE.

Peng Wang, Shuai Bai, Sinan Tan, Shijie Wang, Zhihao Fan, Jinze Bai, Keqin Chen, Xuejing Liu, Jialin Wang, Wenbin Ge, Yang Fan, Kai Dang, Mengfei Du, Xuancheng Ren, Rui Men, Dayiheng Liu, Chang Zhou, Jingren Zhou, and Junyang Lin. 2024. Qwen2-vl: Enhancing vision-language model's perception of the world at any resolution. *CoRR*, abs/2409.12191.

Jen-Her Wu and Yufei Yuan. 2003. Improving searching and reading performance: the effect of highlighting and text color coding. *Information & Management*, 40(7):617–637.

Qifan Yu, Juncheng Li, Longhui Wei, Liang Pang, Wentao Ye, Bosheng Qin, Siliang Tang, Qi Tian, and Yueting Zhuang. 2024. Hallucidoctor: Mitigating hallucinatory toxicity in visual instruction data. In *IEEE/CVF Conference on Computer Vision and Pattern Recognition, CVPR 2024, Seattle, WA, USA, June 16-22, 2024*, pages 12944–12953. IEEE.

Shuo Zhang, Pengjiang Wang, and Wenjun Hou. 2018. Research on font emotion based on semantic difference method. In *International Conference on Human Centered Computing*, pages 304–313. Springer.

Yiyang Zhou, Chenhang Cui, Jaehong Yoon, Linjun Zhang, Zhun Deng, Chelsea Finn, Mohit Bansal, and Huaxiu Yao. 2024. Analyzing and mitigating object hallucination in large vision-language models. In *The Twelfth International Conference on Learning Representations, ICLR 2024, Vienna, Austria, May 7-11, 2024*. OpenReview.net.

Deyao Zhu, Jun Chen, Xiaoqian Shen, Xiang Li, and Mohamed Elhoseiny. 2024. Minigpt-4: Enhancing vision-language understanding with advanced large language models. In *The Twelfth International Conference on Learning Representations, ICLR 2024, Vienna, Austria, May 7-11, 2024*. OpenReview.net.

# A Details on the Font Clustering Algorithm

To effectively organize and analyze the high-dimensional feature vectors of fonts, we adopt a two-step approach comprising dimensionality reduction using Uniform Manifold Approximation and Projection (UMAP) and clustering using K-means. This methodology facilitates the identification of representative fonts by leveraging the complementary strengths of UMAP's non-linear dimensionality reduction and K-means' centroid-based clustering.

High-dimensional feature vectors are often challenging to visualize and cluster due to the "curse of dimensionality" and the complex relationships between features. To address this, we employ **Uniform Manifold Approximation and Projection (UMAP)**(McInnes and Healy, 2018), a state-of-the-art non-linear dimensionality reduction technique known for preserving both local and global structures of high-dimensional data (McInnes and Healy, 2018). Given a set of high-dimensional vectors representing font features:

$$X = \{x_1, x_2, \ldots, x_n\}, \quad x_i \in \mathbb{R}^d,$$

where $n$ denotes the number of fonts and $d$ represents the dimensionality of the feature space, UMAP projects these vectors into a lower-dimensional space $\mathbb{R}^m$ while preserving the topological structure:

$$f : \mathbb{R}^d \to \mathbb{R}^m, \quad Z = f(X),$$

where $Z = \{z_1, z_2, \ldots, z_n\}$ and $m \ll d$. UMAP constructs a weighted k-nearest neighbor graph to model the local relationships between high-dimensional points, optimizing the following cross-entropy objective:

$$C = -\sum_{i \neq j} \left[ p_{ij} \log q_{ij} + (1 - p_{ij}) \log(1 - q_{ij}) \right],$$

where $p_{ij}$ is the conditional probability of $x_i$ being close to $x_j$ in the high-dimensional space, estimated using a Gaussian kernel. $q_{ij}$ is the corresponding probability in the lower-dimensional space, parameterized as a Student's t-distribution to better capture local structures. This optimization preserves the local neighborhood continuity while maintaining the global data manifold, thus ensuring that similar fonts are embedded closely together in the reduced space.

Following dimensionality reduction, the transformed vectors are clustered using **K-means**, a widely-used centroid-based clustering algorithm that minimizes the within-cluster variance. Specifically, the vectors are partitioned into $K = 200$ clusters to capture the diverse stylistic variations present in the font dataset. The objective function of K-means is defined as follows:

$$J = \sum_{k=1}^{K} \sum_{i \in C_k} \|z_i - \mu_k\|^2,$$

where:$C_k$ denotes the set of vectors assigned to cluster $k$. $\mu_k$ is the centroid of cluster $C_k$, calculated as:

$$\mu_k = \frac{1}{|C_k|} \sum_{i \in C_k} z_i.$$

$\|\cdot\|$ represents the Euclidean distance.The K-means algorithm alternates between the following two steps until convergence:

1. **Assignment Step**: Assign each vector to the nearest centroid:

$$C_k = \{z_i : \|z_i - \mu_k\|^2 \leq \|z_i - \mu_j\|^2, \forall j, 1 \leq j \leq K\}$$

2. **Update Step**: Recalculate the centroids as the mean of all vectors in each cluster:

$$\mu_k = \frac{1}{|C_k|} \sum_{i \in C_k} z_i$$

This iterative procedure continues until convergence, yielding 200 distinct clusters. From each cluster, **five representative fonts** are selected based on their proximity to the cluster centroid, ensuring

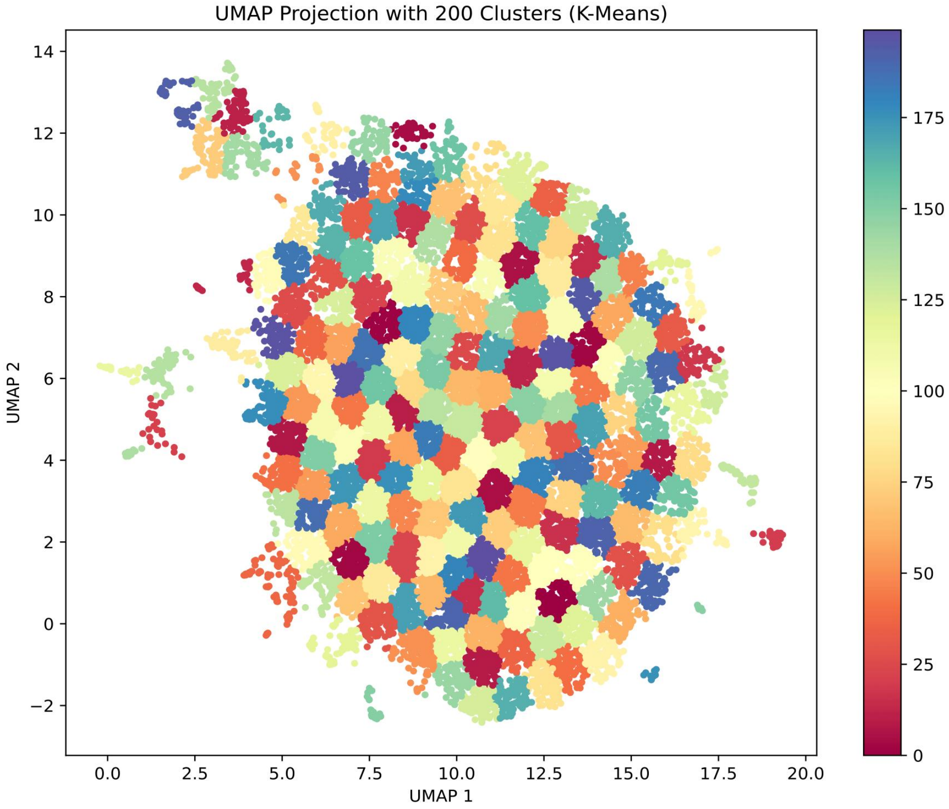

Figure 6: Font clustering result diagram.

that the chosen fonts are central and representative of their respective clusters:

$$F_k = \arg\min_{x \in C_k} \|z_i - \mu_k\|, \quad |F_k| = 5,$$

where $F_k$ denotes the set of five representative fonts from cluster $k$. This process yields a total of **1,000 candidate fonts**, providing a diverse yet concise benchmark set. Finally, the result of kmeans is shown in the figure6.

## B Annotation and Filtering Criteria

The **annotation criteria** are as follows:

1. The bounding box (bbox) should ensure that the corresponding keyword is clearly visible, facilitating subsequent queries about the content within the bbox based on the keyword.
2. The bounding box should align as closely as possible with the original content's location, avoiding discrepancies with the actual key content.
3. When annotating, the size of the bounding box should match the actual content's dimensions, avoiding excessive cropping or expansion.
4. The bounding box should not obscure any crucial information, ensuring that all key content is fully presented.

The **filtering criteria** are as follows:

1. Images with truncated content are filtered out.
2. Images with garbled content, where the corresponding font fails to render ASCII characters, are excluded. Images where the content is unclear or fuzzy (i.e., human-readable keywords are difficult to discern) are removed.
3. During the verification process, three reviewers assess the image, and it is only discarded if all three reviewers agree that the content is unreadable.

## C Evaluation Metrics

Here, $y_i$ denotes the expected answer with spaces removed and $\hat{y}_i$ denotes the generated answer with spaces removed:

1. **ACC:** For each sample:

$$\text{Score}_i = 1 \text{ if } y_i \text{ in } \hat{y}_i, \text{ else } 0.$$

   The overall ACC is:

$$\text{Acc}(Y, \hat{Y}) = \frac{1}{N} \sum_{i=1}^{N} \text{Score}_i(y_i, \hat{y}_i).$$

2. **NED:**

$$\text{NED} = \frac{1}{N} \sum_{i=1}^{N} \frac{\text{EditDistance}(y_i, \hat{y}_i)}{\max(|y_i|, |\hat{y}_i|)}$$

## D Detailed Experiment on Font-based Hallucination

This section primarily provides supplementary details for the experiments in Section 5.1.

In the **Font Style (Plain)** experiment, Roboto, a widely used font from Google Fonts, serves as the base font. To isolate the effect of each dimension, only one dimension is varied at a time, while the others remain at their default values(e.g., size of 20, weight of 400, alignment as left, spacing as 0em, slant as 0, and line-height as 1). The canvas size is set to 1024x256 pixels. We begin with a set of 200 images, each featuring a blank background to eliminate layout interference. Each image contains three lines of text: the first line consists of random numbers, the second line contains random letters, and the third line features a sentence. For each dimension under investigation, variations are applied to these 200 base images. The multimodal large model's task is to recognize and extract all text content from these images. An example can be seen in the top-left corner of the "font variations" box in Figure 7.

In the **Font Style (Scene)** experiment, we select five representative fonts, including both English and Chinese styles. The experimental scenarios cover common numerical applications, such as tracking numbers, ID cards, invoices, and transportation permits. We first collect data from the aforementioned scenarios, then annotate the data with bounding boxes (bbox), removing the original content within the boxes and replacing it with new content, restricting it to numerical data to eliminate language-related factors. The task is to have MLLMs recognize the content within these boxes. Finally, we constructed a dataset consisting of 2,000 Chinese samples and 2,000 English samples.

In the **Font Semantics** experiment, similar to the Font Style (Scene) experiment, we draw specific content on images from various scenarios and task MLLMs with recognizing the content. The key difference is that the applied content undergoes four random format transformations: normal, strikethrough, overlay, and highlight. We select the Roboto font and generate 2,000 data samples for each format to conduct our exploration.

In **Font Sentiment** experiment, We select 1,000 samples from the test set of the `Sentiment140` dataset and render the text using three font styles: a visually neutral font, a horror-themed font, and a visually cheerful font. Those fonts can be seen in Figure 8. The images are then evaluated by MLLMs to determine which emotion is conveyed by texts in the images.

## E Detailed Scores on Subtasks of Benchmark

The table 6 shows the scores of each subset in the benchmark, including VarRec, SemAna, and SentAna. The scores of each subset can be seen from the table. It can be seen that the highest score of VarRec is the model Qwen2-VL-7B, with an accuracy of 62.80%. There are still many models that do not have the ability to recognize long out-of-order texts, with an accuracy rate below 10%.

In the SemAna subset, the main tasks are KIE recognition tasks in the context of documents and invoices. The length of the content to be recognized is not as long as that of the VarRec dataset, so the overall recognition difficulty is relatively low, and the weaker models also have a certain accuracy rate. The highest accuracy rate is also the Qwen2-VL-7B model, with an accuracy rate of 68.19%, beating many models with larger parameters, which also indirectly shows that models with larger parameters are not necessarily more robust to fonts in KIE recognition tasks.

## F Benchmark Models

Table 8 lists all models evaluated in this paper，including the ways in which the institution to which the model belongs has acquired it.

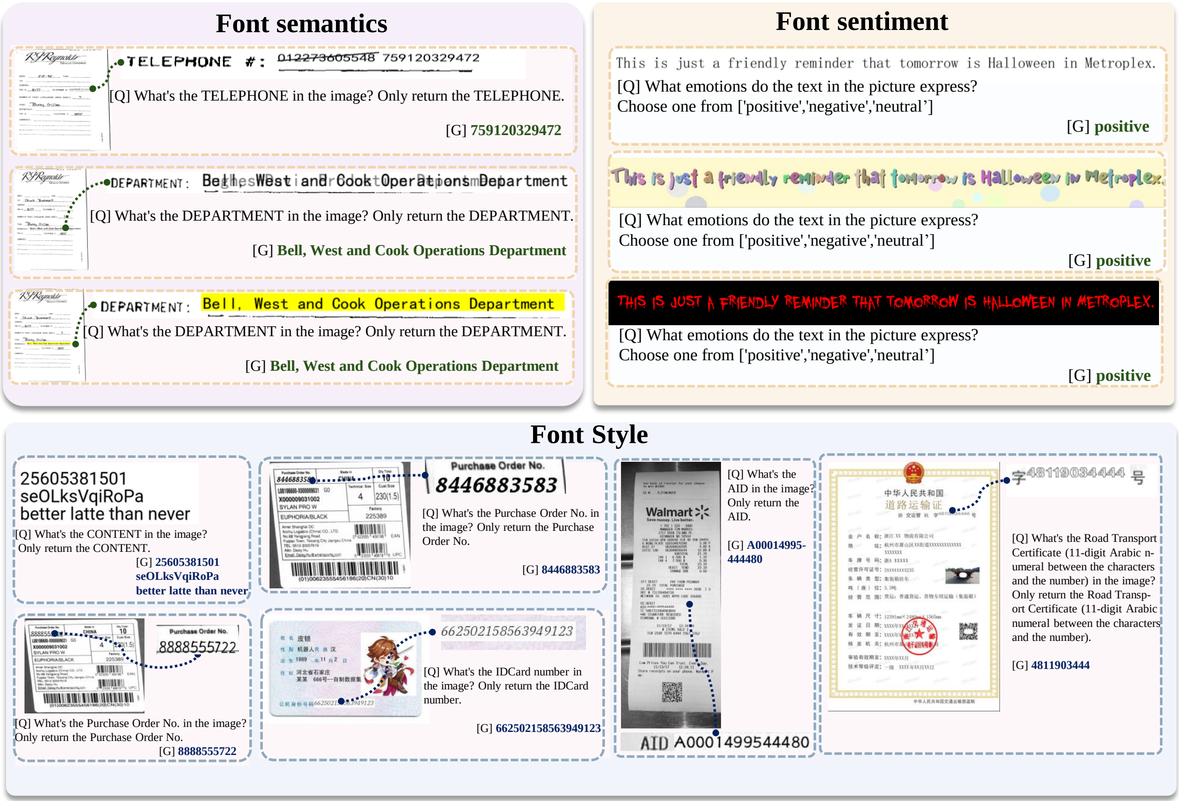

Font semantics

TELEPHONE #: 012273605548 759120329472

[Q] What's the TELEPHONE in the image? Only return the TELEPHONE.

[G] 759120329472

DEPARTMENT: Bell, West and Cook Operations Department

[Q] What's the DEPARTMENT in the image? Only return the DEPARTMENT.

[G] Bell, West and Cook Operations Department

DEPARTMENT: Bell, West and Cook Operations Department

[Q] What's the DEPARTMENT in the image? Only return the DEPARTMENT.

[G] Bell, West and Cook Operations Department

Font sentiment

This is just a friendly reminder that tomorrow is Halloween in Metroplex.

[Q] What emotions do the text in the picture express? Choose one from ['positive','negative','neutral']

[G] positive

This is just a friendly reminder that tomorrow is Halloween in Metroplex.

[Q] What emotions do the text in the picture express? Choose one from ['positive','negative','neutral']

[G] positive

THIS IS JUST A FRIENDLY REMINDER THAT TOMORROW IS HALLOWEEN IN METROPLEX.

[Q] What emotions do the text in the picture express? Choose one from ['positive','negative','neutral']

[G] positive

Font Style

[Q] What's the CONTENT in the image? Only return the CONTENT.

[G] 25605381501 seOLksVqiRoPa better latte than never

[Q] What's the Purchase Order No. in the image? Only return the Purchase Order No.

[G] 8446883583

[Q] What's the AID in the image? Only return the AID.

[G] A00014995-444480

[Q] What's the Road Transport Certificate (11-digit Arabic numeral between the characters and the number) in the image? Only return the Road Transport Certificate (11-digit Arabic numeral between the characters and the number).

[G] 4811903444

[Q] What's the Purchase Order No. in the image? Only return the Purchase Order No.

[G] 8888555722

[Q] What's the IDCard number in the image? Only return the IDCard number.

[G] 662502158563949123

Figure 7: Example images from the font-based hallucination experiment in Section 5.1. [Q] represents the question, and [G] represents the ground truth.

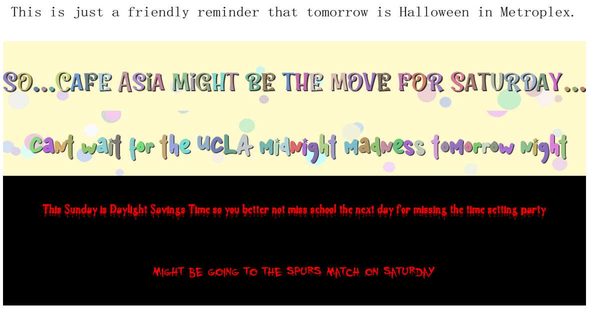

This is just a friendly reminder that tomorrow is Halloween in Metroplex.
SO...CAFE ASIA MIGHT BE THE MOVE FOR SATURDAY...
can't wait for the UCLA midnight madness tomorrow night
This Sunday is Daylight Savings Time so you better not miss school the next day for missing the time setting party
MIGHT BE GOING TO THE SPURS MATCH ON SATURDAY

Figure 8: The fonts used in the images from top to bottom are Neutral Font, Cheerful Font A, Cheerful Font B, Horror-themed Font A, and Horror-themed Font B.

## G Training Configuration Details

We conducted parameter-efficient fine-tuning using **Low-Rank Adaptation (LoRA)** with a rank value of 8 on three vision-language architectures: **LLaVA-1.6-Mistral-7B**, **MiniCPM-V-2.6**, and **Qwen2-VL-7B**. To achieve comprehensive adaptation of multimodal representations, LoRA injections were applied to all linear layers—including attention mechanisms and feed-forward networks—with a base learning rate of $1 \times 10^{-5}$ regulated by cosine decay scheduling and a 10% warmup phase. The training process employed gradient accumulation over 8 steps per device coupled with **FP16** mixed-precision arithmetic. The experiments are all conducted on the A100 for both inference and fine-tuning.

## H Evaluation Samples

Here are some benchmark recognition examples 9, 10, 11, 12. Each example shows the answers of 4 models, namely Qwen2-VL-72B, Qwen2-VL-7B, Minicpm-V-2.6 and GPT4o models.

| **Model** | **VarRec** | **SemAna** | **SentAna** |
|---|---|---|---|
| Qwen2-VL-7B | 0.6280 | 0.6819 | 0.5690 |
| Qwen2-VL-2B | 0.6120 | 0.6798 | 0.5114 |
| Gemini-Pro-1.5 | 0.2680 | 0.6718 | 0.5315 |
| Gemini-Pro-Vision | 0.0480 | 0.6548 | 0.5696 |
| GPT-4o-2024-08-06 | 0.4280 | 0.5717 | 0.6702 |
| MiniCPM-V-2.6 | 0.3640 | 0.5876 | 0.5510 |
| Glm-4v-9B | 0.3440 | 0.5850 | 0.5918 |
| Phi-3-Vision-128k-Instruct | 0.1080 | 0.6244 | 0.4577 |
| InternVL2.5-1B | 0.2160 | 0.6095 | 0.4504 |
| InternVL2.5-2B | 0.2120 | 0.6137 | 0.4136 |
| Qwen2-VL-72B-Instruct | 0.3760 | 0.5637 | 0.6259 |
| InternVL2-4B | 0.1880 | 0.5855 | 0.4597 |
| InternVL2.5-8B | 0.2080 | 0.5690 | 0.5227 |
| InternVL2.5-4B | 0.2240 | 0.5738 | 0.4599 |
| Minimax-01 | 0.2533 | 0.5431 | 0.3305 |
| Pixtral-12B | 0.2960 | 0.4997 | 0.5916 |
| InternVL2-8B | 0.1480 | 0.5328 | 0.4726 |
| InternVL2-1B | 0.1320 | 0.5605 | 0.2608 |
| InternVL2-2B | 0.1160 | 0.5429 | 0.3669 |
| CogVLM2-LLaMA3-19B-Chat | 0.0840 | 0.5003 | 0.5574 |
| LLaMA3.2-90B-Vision-Instruct | 0.0840 | 0.4758 | 0.4947 |
| Phi3.5-Vision-Instruct | 0.1200 | 0.4513 | 0.5091 |
| Ovis1.5-LLaMA3-8B | 0.1200 | 0.4156 | 0.4541 |
| LLaVA-V1.6-Vicuna-7B-hf | 0.0120 | 0.4182 | 0.4744 |
| LLaMA3-LLaVA-Next-8B-hf | 0.0240 | 0.3953 | 0.4856 |
| LLaVA-V1.6-Mistral-7B | 0.0160 | 0.3937 | 0.4567 |
| LLaMA3.2-11B-Vision-Instruct | 0.1440 | 0.3031 | 0.3077 |
| Deepseek-VL-7B-Chat | 0.0760 | 0.2339 | 0.4026 |
| InstructBLIP-Vicuna-7B | 0.0000 | 0.0027 | 0.3285 |
| BLIP-VQA-Base | 0.0000 | 0.0000 | 0.2844 |

Table 6: Detailed ACC Scores of MLLMs on Three Subtasks

| **Model** | **VarRec** | **SemAna** |
|---|---|---|
| Qwen2-VL-7B | 0.0663 | 0.2048 |
| Qwen2-VL-2B | 0.1206 | 0.2673 |
| Gemini-Pro-1.5 | 0.1040 | 0.2061 |
| Gemini-Pro-Vision | 0.3887 | 0.2468 |
| GPT-4o-2024-08-06 | 0.0920 | 0.2821 |
| MiniCPM-V-2.6 | 0.1017 | 0.2706 |
| Glm-4v-9B | 0.1942 | 0.7000 |
| Phi-3-Vision-128k-Instruct | 0.8270 | 0.2897 |
| InternVL2.5-1B | 0.1776 | 0.2498 |
| InternVL2.5-2B | 0.1777 | 0.2468 |
| Qwen2-VL-72B-Instruct | 0.2001 | 0.2880 |
| InternVL2-4B | 0.2330 | 0.2852 |
| InternVL2.5-8B | 0.1619 | 0.2611 |
| InternVL2.5-4B | 0.1731 | 0.2603 |
| Minimax-01 | 0.1225 | 0.3095 |
| Pixtral-12B | 0.1302 | 0.3307 |
| InternVL2-8B | 0.1910 | 0.4544 |
| InternVL2-1B | 0.2390 | 0.3386 |
| InternVL2-2B | 0.2965 | 0.2826 |
| CogVLM2-LLaMA3-19B-Chat | 0.7858 | 0.8073 |
| LLaMA3.2-90B-Vision-Instruct | 0.8038 | 0.5234 |
| Phi3.5-Vision-Instruct | 0.8006 | 0.4282 |
| Ovis1.5-LLaMA3-8B | 0.1671 | 0.3560 |
| LLaVA-V1.6-Vicuna-7B-hf | 0.5810 | 0.3567 |
| LLaMA3-LLaVA-Next-8B-hf | 0.7222 | 0.4786 |
| LLaVA-V1.6-Mistral-7B | 0.8612 | 0.7885 |
| LLaMA3.2-11B-Vision-Instruct | 0.6980 | 0.6670 |
| Deepseek-VL-7B-Chat | 0.5890 | 0.9248 |
| InstructBLIP-Vicuna-7B | 0.9314 | 0.9122 |
| BLIP-VQA-Base | 0.9565 | 0.9314 |

Table 7: Detailed edit distance Scores of MLLMs on Two Subtasks

| **Model** | **Creator** | **Access** |
|---|---|---|
| Qwen2-VL-7B | Alibaba | Weights |
| Qwen2-VL-2B | Alibaba | Weights |
| Gemini-Pro-1.5 | Google | API |
| Gemini-Pro-Vision | Google | API |
| GPT-4o | OpenAI | API |
| MiniCPM-V-2.6 | OpenBMB | Weights |
| Glm-4v-9B | Zhipu AI | Weights |
| Phi-3-Vision-128k-Instruct | Microsoft | Weights |
| InternVL2.5-1B | Shanghai AI Lab | Weights |
| InternVL2.5-2B | Shanghai AI Lab | Weights |
| Qwen2-VL-72B-Instruct | Alibaba | API |
| InternVL2-4B | Shanghai AI Lab | Weights |
| InternVL2.5-8B | Shanghai AI Lab | Weights |
| InternVL2.5-4B | Shanghai AI Lab | Weights |
| Minimax-01 | Minimax | API |
| Pixtral-12B | Mistral AI | API |
| InternVL2-8B | Shanghai AI Lab | Weights |
| InternVL2-1B | Shanghai AI Lab | Weights |
| InternVL2-2B | Shanghai AI Lab | Weights |
| CogVLM2-LLaMA3-19B-Chat | Zhipu AI | Weights |
| LLaMA3.2-90B-Vision-Instruct | Meta | API |
| Phi3.5-Vision-Instruct | Microsoft | Weights |
| Ovis1.5-LLaMA3-8B | Alibaba | Weights |
| LLaVA-V1.6-Vicuna-7B-hf | UW–Madison | Weights |
| LLaMA3-LLaVA-Next-8B-hf | UW–Madison | Weights |
| LLaVA-V1.6-Mistral-7B | UW–Madison | Weights |
| LLaMA3.2-11B-Vision-Instruct | Meta | API |
| Deepseek-VL-7B-Chat | DeepSeek | Weights |
| InstructBLIP-Vicuna-7B | Salesforce | Weights |
| BLIP-VQA-Base | Salesforce | Weights |

Table 8: Models evaluated in this paper

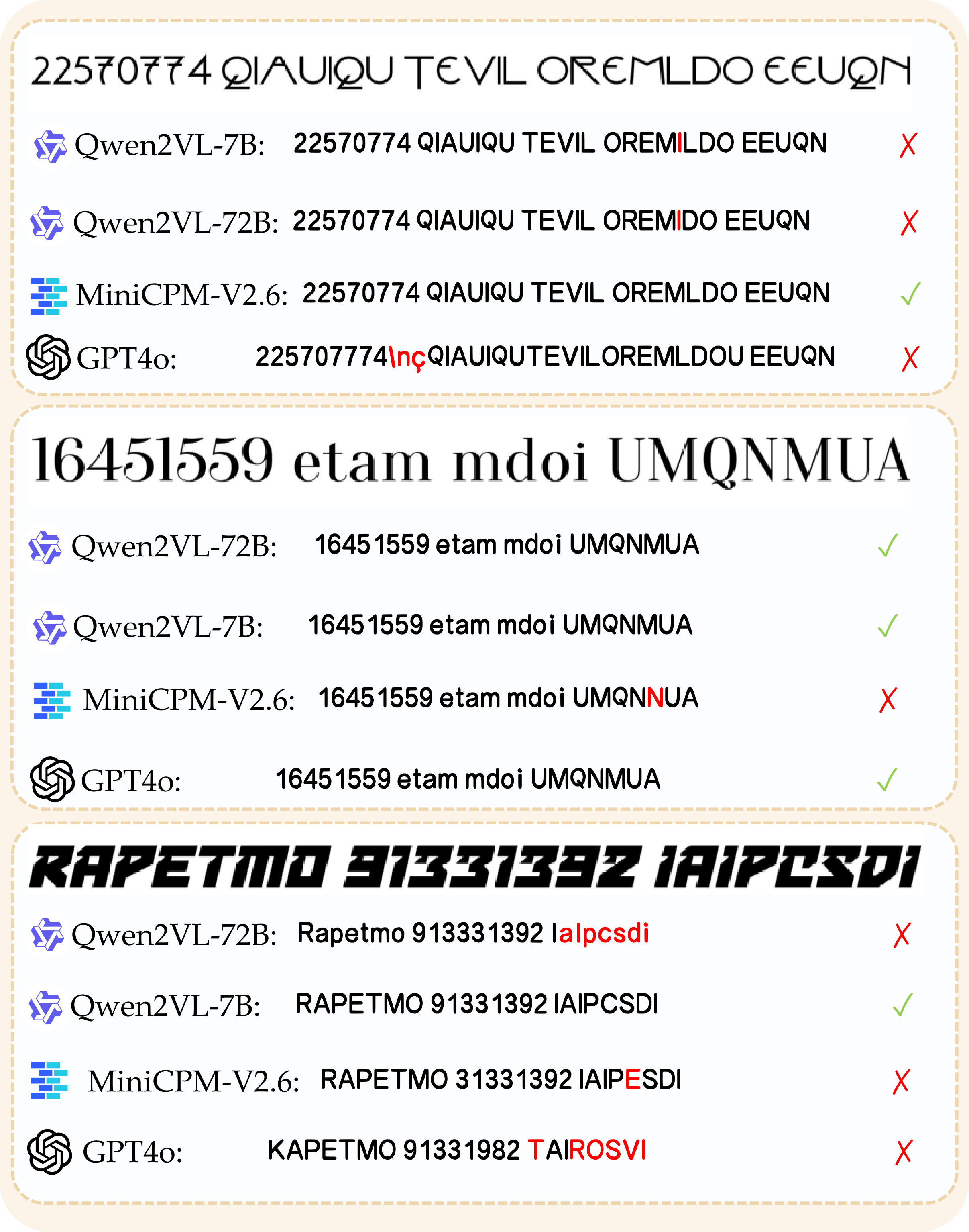
22570774 QIAUIQU TEVIL OREMLDO EEUQN
Qwen2VL-7B: 22570774 QIAUIQU TEVIL OREMILDO EEUQN ✗
Qwen2VL-72B: 22570774 QIAUIQU TEVIL OREMIDO EEUQN ✗
MiniCPM-V2.6: 22570774 QIAUIQU TEVIL OREMLDO EEUQN ✓
GPT4o: 225707774\nçQIAUIQUTEVILOREMLDOU EEUQN ✗
16451559 etam mdoi UMQNMUA
Qwen2VL-72B: 16451559 etam mdoi UMQNMUA ✓
Qwen2VL-7B: 16451559 etam mdoi UMQNMUA ✓
MiniCPM-V2.6: 16451559 etam mdoi UMQNNUA ✗
GPT4o: 16451559 etam mdoi UMQNMUA ✓
RAPETMO 91331392 IAIPCSDI
Qwen2VL-72B: Rapetmo 913331392 lalpcsdi ✗
Qwen2VL-7B: RAPETMO 91331392 IAIPCSDI ✓
MiniCPM-V2.6: RAPETMO 31331392 IAIPESDI ✗
GPT4o: KAPETMO 91331982 TAIROSVI ✗

Figure 9: Some examples from the VarRec dataset, where the red font shows the inconsistency between the model's answer and the correct answer. As shown in the figure, due to changes in font style, there may be some recognition illusions, such as the presence of confusing characters, such as the 'L' character in example 1, which the model may recognize as 'I', and the 'M' character in example 2, which may be recognized as 'N'.

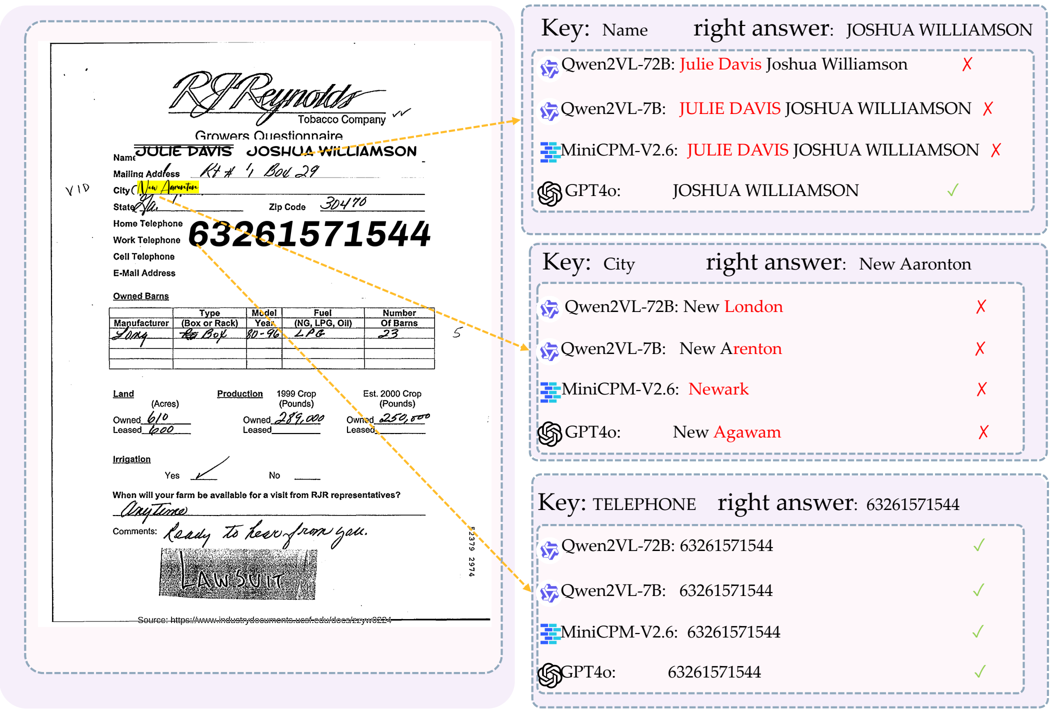

RJReynolds Tobacco Company

Growers Questionnaire

Name ~~JULIE DAVIS~~ JOSHUA WILLIAMSON

Mailing Address Rt # 1 Box 29

VID City (New Aaronton

State Ga. Zip Code 30470

Home Telephone 63261571544

Work Telephone

Cell Telephone

E-Mail Address

Owned Barns

| Manufacturer | Type<br>(Box or Rack) | Model<br>Year | Fuel<br>(NG, LPG, Oil) | Number<br>Of Barns |
|---|---|---|---|---|
| Long | ~~Ra~~ Box | 80-96 | LPG | 23 |
| | | | | |
| | | | | |
| | | | | |

5

Land (Acres)

Owned 610
Leased 600

Production 1999 Crop (Pounds)

Owned 289,000
Leased

Est. 2000 Crop (Pounds)

Owned 250,000
Leased

Irrigation

Yes ✓ No ____

When will your farm be available for a visit from RJR representatives?

AnyTime

Comments: Ready to hear from you.

LAWSUIT

52379 2974

Source: https://www.industrydocuments.ucsf.edu/docs/zzyw0224

Key: Name right answer: JOSHUA WILLIAMSON

Qwen2VL-72B: Julie Davis Joshua Williamson ✗

Qwen2VL-7B: JULIE DAVIS JOSHUA WILLIAMSON ✗

MiniCPM-V2.6: JULIE DAVIS JOSHUA WILLIAMSON ✗

GPT4o: JOSHUA WILLIAMSON ✓

Key: City right answer: New Aaronton

Qwen2VL-72B: New London ✗

Qwen2VL-7B: New Arenton ✗

MiniCPM-V2.6: Newark ✗

GPT4o: New Agawam ✗

Key: TELEPHONE right answer: 63261571544

Qwen2VL-72B: 63261571544 ✓

Qwen2VL-7B: 63261571544 ✓

MiniCPM-V2.6: 63261571544 ✓

GPT4o: 63261571544 ✓

Figure 10: An example from the SemAna dataset. In this example, not only will various fonts be introduced, but also some semantic tasks such as overlay, highlight, and stricthrough will be added. In this case, there are issues such as confusion between uppercase and lowercase, incorrect recognition of the key as a whole, and errors in character-level recognition of the key, etc.

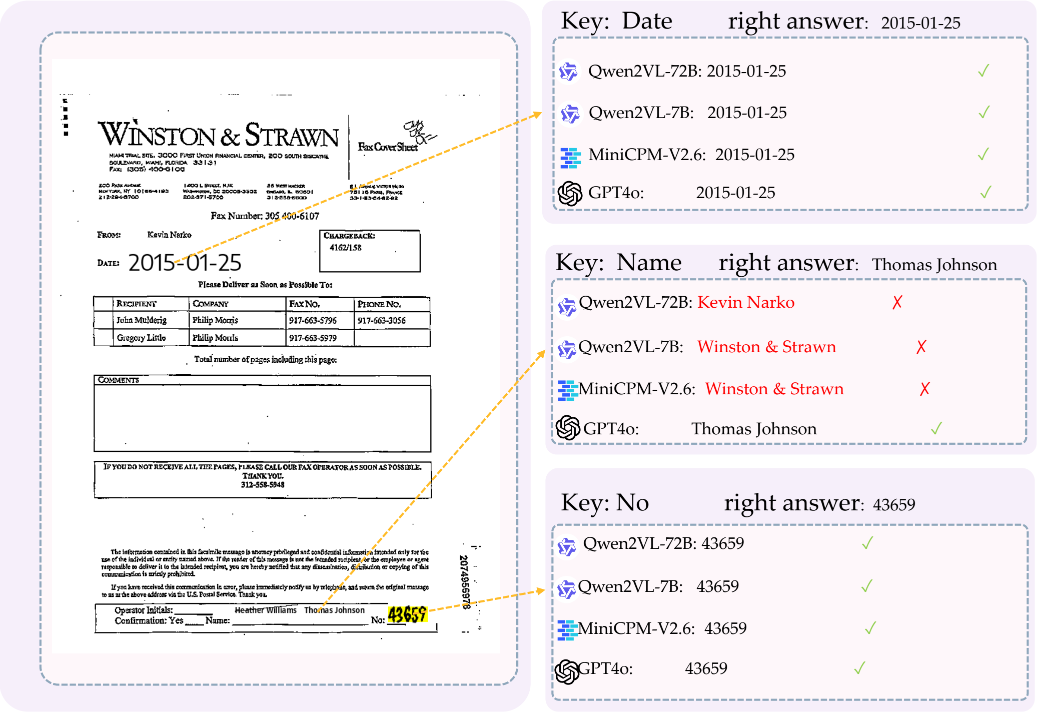

WINSTON & STRAWN

MIAMI TRIAL SITE, 3000 FIRST UNION FINANCIAL CENTER, 200 SOUTH BISCAYNE
BOULEVARD, MIAMI, FLORIDA 33131
FAX: (305) 400-6106

200 PARK AVENUE
NEW YORK, NY 10166-4193
212-294-6700

1400 L STREET, N.W.
WASHINGTON, DC 20005-3502
202-371-5700

35 WEST WACKER
CHICAGO, IL 60601
312-558-5600

21 AVENUE VICTOR HUGO
75116 PARIS, FRANCE
33-1-53-64-82-82

Fax Cover Sheet

Fax Number: 305 400-6107

FROM: Kevin Narko

DATE: 2015-01-25

CHARGEBACK:
4162/158

Please Deliver as Soon as Possible To:

| | RECIPIENT | COMPANY | FAX NO. | PHONE NO. |
|---|---|---|---|---|
| | John Mulderig | Philip Morris | 917-663-5796 | 917-663-3056 |
| | Gregory Little | Philip Morris | 917-663-5979 | |

Total number of pages including this page:

COMMENTS

IF YOU DO NOT RECEIVE ALL THE PAGES, PLEASE CALL OUR FAX OPERATOR AS SOON AS POSSIBLE.
THANK YOU.
312-558-5948

The information contained in this facsimile message is attorney privileged and confidential information intended only for the use of the individual or entity named above. If the reader of this message is not the intended recipient, or the employee or agent responsible to deliver it to the intended recipient, you are hereby notified that any dissemination, distribution or copying of this communication is strictly prohibited.

If you have received this communication in error, please immediately notify us by telephone, and return the original message to us at the above address via the U.S. Postal Service. Thank you.

Operator Initials: ________ ~~Heather Williams~~ Thomas Johnson
Confirmation: Yes ____ Name: ______________________ No: 43659

2074956978

Key: Date right answer: 2015-01-25

Qwen2VL-72B: 2015-01-25 ✓

Qwen2VL-7B: 2015-01-25 ✓

MiniCPM-V2.6: 2015-01-25 ✓

GPT4o: 2015-01-25 ✓

Key: Name right answer: Thomas Johnson

Qwen2VL-72B: Kevin Narko ✗

Qwen2VL-7B: Winston & Strawn ✗

MiniCPM-V2.6: Winston & Strawn ✗

GPT4o: Thomas Johnson ✓

Key: No right answer: 43659

Qwen2VL-72B: 43659 ✓

Qwen2VL-7B: 43659 ✓

MiniCPM-V2.6: 43659 ✓

GPT4o: 43659 ✓

Figure 11: Another example from the SemAna dataset: In the name field recognition task in this example, many models identify incorrect fields and do not account for the interference caused by strikethrough.

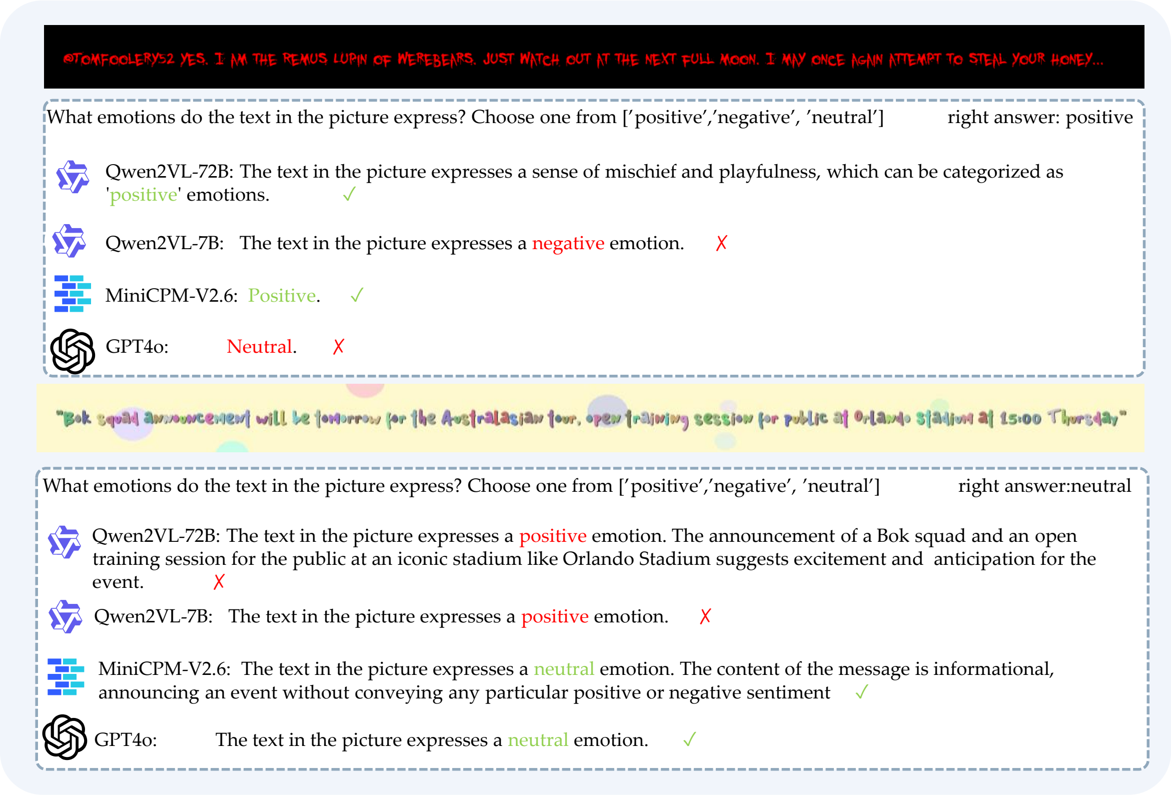

@TOMFOOLERY52 YES. I AM THE REMUS LUPIN OF WEREBEARS. JUST WATCH OUT AT THE NEXT FULL MOON. I MAY ONCE AGAIN ATTEMPT TO STEAL YOUR HONEY...

What emotions do the text in the picture express? Choose one from ['positive','negative', 'neutral'] right answer: positive

Qwen2VL-72B: The text in the picture expresses a sense of mischief and playfulness, which can be categorized as 'positive' emotions. ✓

Qwen2VL-7B: The text in the picture expresses a negative emotion. ✗

MiniCPM-V2.6: Positive. ✓

GPT4o: Neutral. ✗

"Bok squad announcement will be tomorrow for the Australasian tour, open training session for public at Orlando stadium at 15:00 Thursday"

What emotions do the text in the picture express? Choose one from ['positive','negative', 'neutral'] right answer:neutral

Qwen2VL-72B: The text in the picture expresses a positive emotion. The announcement of a Bok squad and an open training session for the public at an iconic stadium like Orlando Stadium suggests excitement and anticipation for the event. ✗

Qwen2VL-7B: The text in the picture expresses a positive emotion. ✗

MiniCPM-V2.6: The text in the picture expresses a neutral emotion. The content of the message is informational, announcing an event without conveying any particular positive or negative sentiment ✓

GPT4o: The text in the picture expresses a neutral emotion. ✓

Figure 12: An example from the SentAna dataset. The text content in the example above is "@ TomFoolery23 Yes, I am the Remus Lupin of werebiers. Just watch out at the next full moon. I may once again attend to steam your honey...". This sentence references the character Remus Lupin from the Harry Potter series, who is a werewolf. Here, someone humbly refers to themselves as the 'werebier version of Lupin' and enjoyable mentions that they might try to steam honey during the next full moon. Clearly, it's a joke with a question. However, some models has identified a neutral, or even negative sentiment. The text content in the example below is "Book special announcement will be tomorrow for the Australian tour, open training session for public at Orlando stadium at 15:00 Thursday." This is an activity description without any specific emotions, and the answer is neutral, but some models answer with positive emotions.